# [1]The 5th- and 7th-order 2D Raman spectroscopy for intramolecular vibrational modes

Yoshitaka Tanimura

*Institute for Molecular Science and the Graduate University for Advanced Studies*
*Myodaiji, Okazaki, Aichi 444-8585, JAPAN*

**Abstract.** We calculated the 3rd-, 5th-, and 7th-order Raman signals for an Iodine dimer in the condensed phase, which was modeled by a Morse potential coupled to a heat bath. It is shown that the 5th- and 7th-order signals are very sensitive to the anharmonicity of the potential and useful to study intramolecular vibrational modes. In the case of harmonic vibrational modes, the 5th- and 7th-order signals are the function of both the linear and nonlinear linear coordinate dependence of the polarizability, whereas the present case they are the function of the linear coordinate dependence of the polarizability. Thus, the signals in the present case are expected to be much stronger than in the harmonic case. We also showed that the 7th-order 2D signal for a harmonic system with a nonlinear system-bath interaction, which is a possible model of an inhomogeneously distributed molecular-vibrational system, depends in the lowest order on the nonlinear coordinate dependence of the polarizability and is useful to see the effects of the inhomogeneity, in cases where the 5th-order 2D signals were very weak.

## I. INTRODUCTION

The delineation of the vibrational line shapes of molecules in condensed phases has been the subject of numerous experimental and theoretical studies. Although models of a solvent's vibrational and orientational dynamics can be tested against infrared and Raman studies, there are still ambiguities. For example, one usually assigned the spectral density obtained from experiments to the spectral distribution of the harmonic oscillators modes, but this may not be true for orientational dynamics because of the anharmonicity of a potential. In order to confirm the validity of models, one needs to have experiments to compare the difference. The fifth-order two-dimensional vibrational spectroscopy (5th-order 2D Raman spectroscopy) is such an example (1).

CP503, Two-Dimensional Correlation Spectroscopy, edited by Y. Ozaki and I. Noda 2000 AIP

It was proposed to experimentally separate the inhomogeneous distribution of slowly varying parameters, for example of local liquid configurations, from the total spectral density. This experiment uses two pairs of excitation pulses, followed by a probe pulse and therefore has two time variables. By plotting the fifth-order signal as function of these delay times, we obtain the two-dimensional profile of the signal. Although the 2D Raman experiment was proposed to study inhomogeneity, the same technique can be used to access various dynamical information of molecules in condensed phases, such as the anharmonicity of potentials (2, 3) and the coupling mechanism between different vibrational modes (4, 5). In this paper, we present the 5th and 7th order 2D Raman spectra of the intravibrational mode of an Iodine dimer in the condensed phase, which is modeled by a Morse potential coupled to a heat bath. We focus in particular on the sensitivity of the 5th and 7th order 2D Raman response to the potential surface and the system-bath coupling strength. It is shown that the signals from the intravibronic anharmonic modes may be much stronger than the harmonic modes. For anharmonic potential, the leading contribution to the 5th- and 7th-order 2D Raman signals depends on the linear coordinate dependence of the polarizability, whereas those from harmonic potentials are nonlinear. The 7th-order 2D Raman signal from a harmonic system with a nonlinear system-bath interaction, which is a possible model of an inhomogeneously distributed molecular-vibrational system, is also discussed. It is shown that such signal exhibits Raman echo like peaks in the stochastic overdamped case.

## II. THE SYSTEM AND CORRELATION FUNCTIONS

We employed a system-bath Hamiltonian expressed as

$$H = \frac{P^2}{2M} + U(Q) + \sum_n \left[ \frac{p_n^2}{2m_n} + \frac{m_n \omega_n^2}{2} \left( x_n - \frac{F_n(Q)}{m_n \omega_n^2} \right)^2 \right], \tag{1}$$

where $P$ and $Q$ are the primary nuclear momentum and coordinate, $p_n$ and $x_n$ are the momenta and coordinates of the bath oscillators with the frequency $\omega_n$ and the mass $m_n$, respectively. In Sec. II and III, we consider a linear-linear system-bath interaction, i.e. $F_n(Q)=c_nQ$ with a coupling strength $c_n$. A quadratic case, $F_n(Q)=c_nQ^2$, which can be interpreted as a half-breed of the Brownian and stochastic models, will be discussed in Sec. IV to connect the 7th-order 2D Raman theory to the Raman echo one. The character of the bath is determined by the spectral density $J(\omega)$. Here, we assume

$$J(\omega) \equiv \sum_n \left( \frac{c_n^2}{2m_n\omega_n^2} \right) \delta(\omega - \omega_n) = \frac{M\zeta\omega}{2\pi}. \tag{2}$$

The molecular system is interacting with an off-resonant laser field, $E(\boldsymbol{r}, t)$, where $\boldsymbol{r}$ is the position of the molecular system. We consider the 3rd-, 5th- and 7th-order off-resonant experiments. The system first interacts with $N$ pairs of pulses for the $2N$+1th order optical process, which have the same time profile $E_j(t)$ ($N \geq j$), but different wave vectors $\boldsymbol{k}_j$ and $\boldsymbol{k}_j'$ for the $j$th pair of pulse, respectively. The last pulse $\boldsymbol{k}_T$ is the probe that generates the signal (1). The effective Hamiltonian including laser interaction is then given by $H_{\text{eff}}=H-E^2(\boldsymbol{r}, t)\alpha(Q)$, where $\alpha(Q)$ is the coordinate dependent polarizability. We consider the laser pulses in the following three cases:

$$\begin{aligned}
&\text{(I) } E_1(t) = \delta(t), \quad E_T(t) = \delta(t - \tau_1), \\
&\text{(II) } E_1(t) = \delta(t), \quad E_2(t) = \delta(t - \tau_1), \quad E_T(t) = \delta(t - \tau_1 - \tau_2), \\
&\text{(III) } E_1(t) = \delta(t), \quad E_2(t) = \delta(t - \tau_1), \quad E_3(t) = \delta(t - \tau_1), \quad E_T(t) = \delta(t - \tau_1 - \tau_2).
\end{aligned} \tag{3}$$

Note that the pulse configuration for the 7th-order case (III) is the same as the Raman echo experiment (6,7), however, the model in this section does not show echo peaks because the nature of the present Brownian motion model is very different from the stochastic model which was used to derive the Raman echo theory (6). Here, we use such signal for 2D analysis. The signal for the above three cases are, respectively, expressed by the response function

$$\begin{aligned}
&\text{(I) } R^{(3)}(\tau_1) = \frac{i}{\hbar}\left\langle [\alpha(Q(\tau_1)), \alpha(Q(0))] \right\rangle, \\
&\text{(II) } R^{(5)}(\tau_2, \tau_1) = -\frac{1}{\hbar^2}\left\langle [[\alpha(Q(\tau_1 + \tau_2)), \alpha(Q(\tau_1))], \alpha(Q(0))] \right\rangle, \\
&\text{(III) } R^{(7)}(\tau_2, 0, \tau_1) = -\frac{i}{\hbar^3}\left\langle [[[\alpha(Q(\tau_1 + \tau_2)), \alpha(Q(\tau_1))], \alpha(Q(\tau_1))], \alpha(Q(0))] \right\rangle,
\end{aligned} \tag{4}$$

as $I^{(2N+1)}(\tau_1, \ldots, \tau_N) = |R^{(2N+1)}(\tau_N, \ldots, \tau_1)|^2$. The polarizability is assumed to be

$$\alpha(Q) = \alpha_0 + \alpha_1 Q + \alpha_2 Q^2 + \alpha_3 Q^3 + \ldots \tag{5}$$

In Sec. III, we consider the cases of (1) the harmonic potential and (2) the Morse potential:

$$\text{(1)} \quad U(Q) = \frac{1}{2} M\omega_0^2 Q^2, \qquad \text{(2)} \quad U(Q) = E_c\left(1 - e^{-aQ}\right)^2, \tag{6}$$

where $E_c$ and $a$ are the dissociation energy and the curvature of the potential, respectively. For a harmonic case, the signals are calculated analytically as

$$\begin{aligned}
&\text{(I) } R^{(3)}(\tau_1) = \frac{2i\alpha_1^2}{\hbar} C''(\tau_1), \\
&\text{(II) } R^{(5)}(\tau_2, \tau_1) = \frac{4\alpha_1^2\alpha_2}{\hbar^2} C''(\tau_2)\left[C''(\tau_1) + C''(\tau_1+\tau_2)\right], \\
&\text{(III) } R^{(7)}(\tau_2, 0, \tau_1) = \frac{16i\alpha_1^2\alpha_2^2}{\hbar^3} C''(\tau_1)C''^2(\tau_2),
\end{aligned} \tag{7}$$

where we have introduced the anti-correlation function of the Brownian oscillator

$$C''(\tau) \equiv \left\langle [Q(\tau), Q] \right\rangle = \frac{\omega_0}{\sqrt{\omega_0^2 - \gamma^2/4}} \exp\left(\frac{-\zeta\tau}{2}\right) \sin\left(\sqrt{\omega_0^2 - \frac{\gamma^2}{4}}\ \tau\right). \tag{8}$$

As can be seen from the prefactors of Eq.(7), the 5th and 7th-order signals arise from the correlation functions in even order of $Q$, such as $\alpha_1^2\alpha_2$<[[$Q^2(t')$, $Q(t)$], $Q$]> in the fifth-order. This is because the lowest order correlation, such as $\alpha_1^3$<[[$Q(t')$, $Q(t)$], $Q$]> will be vanished due to the fact that <[$Q(t')$, $Q(t)$]> becomes c-number. This is one reason that the Brownian oscillator model does not exhibit Raman echo like peaks in the 7th-order, as we will discuss in Sec. IV. Here, we use the 7th-order signal not for echo experiment but for two-dimensional analysis.

## III. HIGHER-ORDER RAMAN SIGNALS OF HARMONIC AND MORSE OSCILATOR SYSTEMS

We calculated the signals for a Morse potential using the quantum Fokker-Planck equation (3, 8). We set $E_c$=12436 (cm$^{-1}$), $a$=1.868 as the ground state of the $I_2$ molecule. The fundamental frequency is then given by $\omega_0$=209.8 (cm$^{-1}$). The harmonic potential is also set to have the same fundamental frequency. The polarizability is assumed to be $\alpha_1$=1 and $\alpha_2$=0.01. Since the procedure is parallel to (3), here we show the results only. Note that the calculations presented in (3) were for $Cs_2$ molecule and were limited to the 3rd and 5th order, but here we calculate the signals for $I_2$ molecule including the 7th-order. In the following, we use three values of the system-bath coupling strength (friction) $\zeta$=0.1$\omega_0$ (weak), $\zeta$=0.5$\omega_0$ (intermediate), and $\zeta$=$\omega_0$ (strong) for the fixed temperature $T$=300[K].

## The third-order signal

Figure 1 displays the Fourier transform of the 3rd order signal,

$$R^{(3)}(\omega) = \mathrm{Im}\left\{\int_0^\infty dt\, e^{-i\omega t} R^{(3)}(t)\right\}, \tag{9}$$

for (1) the harmonic potential case and (2) the Morse potential case for a different coupling strength (a) $\zeta=0.1\omega_0$, (b) $\zeta=0.5\omega_0$, and (c) $\zeta=\omega_0$. For a weak damping (a) and (b), the peaks in the Morse potential case slightly shift to red because, the energy between adjacent levels decreases with increasing quantum number and, at this temperatures, many levels become populated, showing up in a smaller effective frequency. Such shifts become smaller for an overdamped case (c), because of the lack of the coherent oscillation. In any case, however, the differences between the harmonic and Morse potential are very small and are impossible to distinguish.

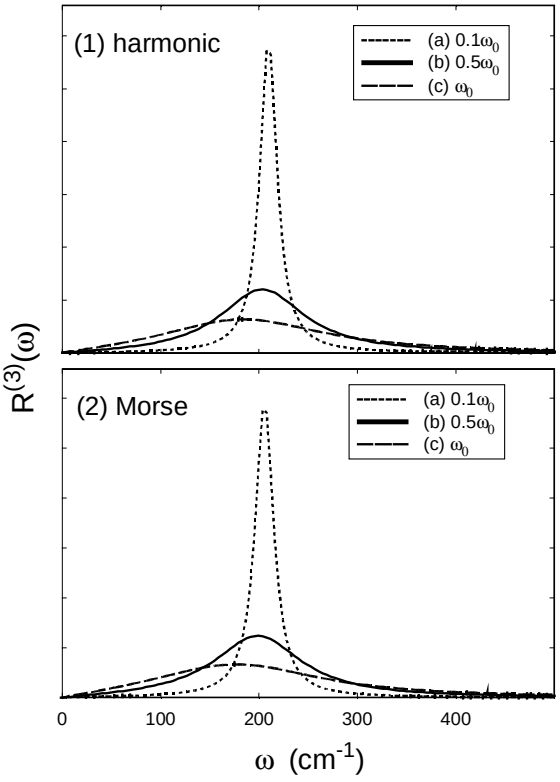


**FIGURE 1.** The third-order Raman signals for (1) the harmonic case and (2) the Morse case for different coupling strength (a) $\zeta=0.1\omega_0$, (b) $\zeta=0.5\omega_0$, and (c) $\zeta=\omega_0$. Two cases are almost identical beside small peak shift.

## The fifth-order signal

Next, we present the fifth-order off-resonant 2D signals, $I^{(5)}(\tau_1, \tau_2)=|R^{(5)}(\tau_2, \tau_1)|^2$, for different coupling strength (a) $\zeta=0.1\omega_0$, (b) $\zeta=0.5\omega_0$, and (c) $\zeta=\omega_0$. Figures 2(1a)-(1c) are the 2D signals for the harmonic potential. As was discussed in (2), the decay rate of peaks in $\tau_1$ direction is $-\zeta$, whereas in the $\tau_2$ direction consists of three components with the decay rates $-\zeta$, $-2\zeta$, and $-3/2\zeta$, respectively. Thus, the decay in the $\tau_2$ direction is faster than $\tau_1$ direction. Figures 2(2a)-(2c) are for the Morse potential. As was mentioned in Sec. II, the dominant contribution of the signal in the Morse case is the lowest order term, $\alpha_1^3<[[Q(\tau_1+\tau_2), Q(\tau_1)], Q]>$, whereas $\alpha_1^2\alpha_2<[[Q^2(\tau_1+\tau_2), Q(\tau_1)], Q]>$, etc. in the harmonic case. Thereby the profile of the signal is very different from that of the harmonic case even in the overdamped cases (see (1c) and (2c)), which was impossible to distinguish from the 3rd-order experiments.

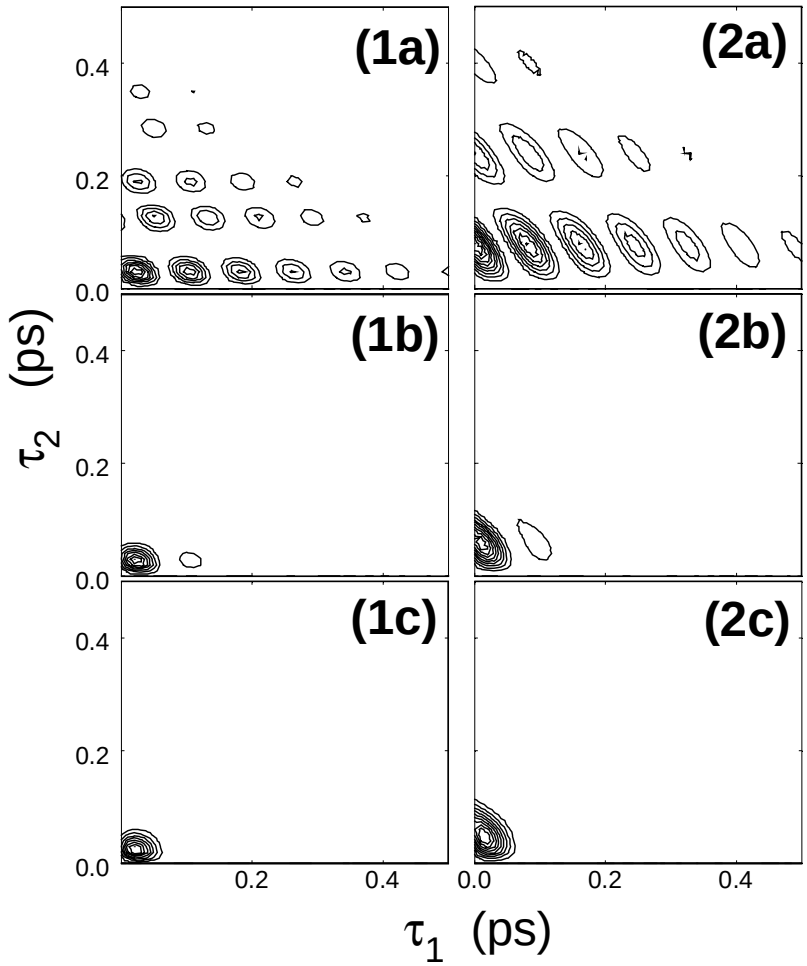


**FIGURE 2.** The fifth-order 2D Raman signal for (1) the harmonic potential and (2) the Morse potential for different coupling strength. The differences between the harmonic and Morse cases are now clear.

## The seventh-order signal

Now we present the seventh-order 2D signal, $I^{(7)}(\tau_1, \tau_2)=|R^{(7)}(\tau_2, 0, \tau_1)|^2$. Like in the fifth-order case, the leading contribution of a signal for the Morse potential is $\alpha_1^4<[[Q(\tau_1+\tau_2), Q^2(\tau_1)], Q]>$, whereas $\alpha_1^2\alpha_2^2<[[Q^2(\tau_1+\tau_2), Q^2(\tau_1)], Q^2]>$ for the harmonic one. Thus, the time-dependence of signal is very different for these two cases. It was shown that the 5th-order experiment is useful to detect 3rd-order anharmonicity, whereas the 7th-order experiment is sensitive to the 4th-order one (2). This indicates that, by convening the results of different order of experiments, we can reconstruct the molecular potential in the condensed phase. Since the perturbation of a Brownian heat bath does not modulate the energy levels of potential, here we do not observe Raman echo signal in $\tau_1=\tau_2$ direction. In the next section, we will introduce a model to discuss a relation between the present theory and Raman echo theory.

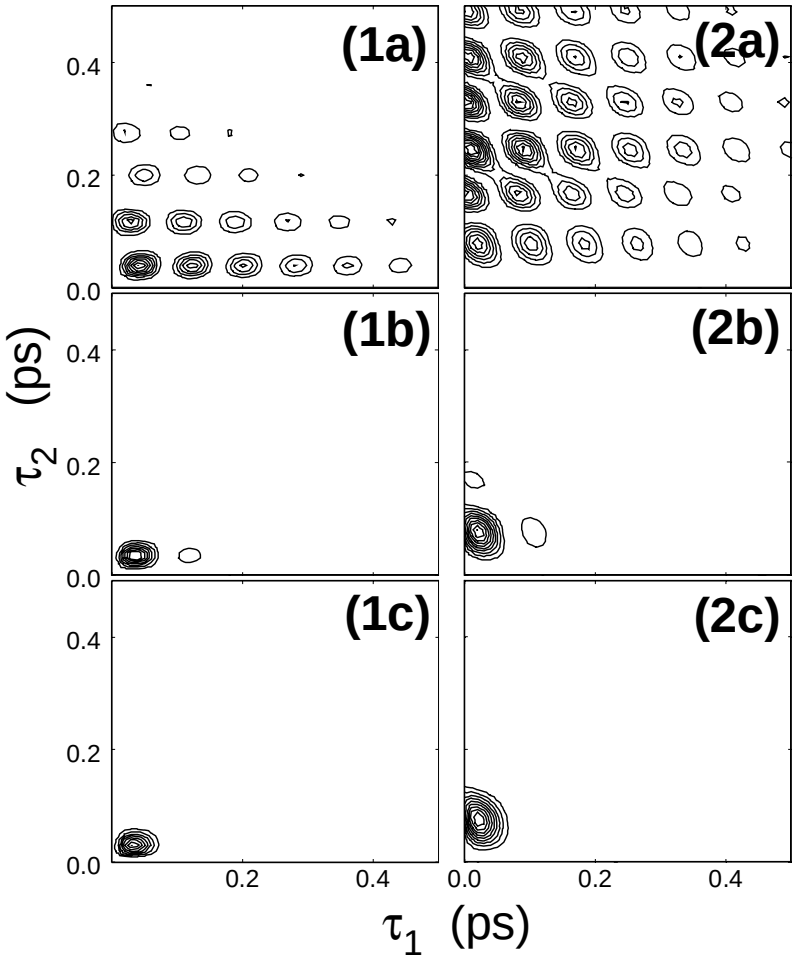


**FIGURE 3.** The 7th-order 2D Raman signal for (1) the harmonic potential and (2) the Morse potential for different coupling strength.

## IV. THE SEVENTH-ORDER SIGNAL OF FREQUENCY MODULATION MODEL

As was discussed above, we cannot observe an echo like signal from a Brownian oscillator, since the stochastic perturbation of vibrational levels is essential to have the echo, but the system-bath interaction of the Brownian model does not produces level fluctuation but friction on the system. Indeed, one never observed the Raman echo signal for the intermolecular vibrational modes, where the Brownian oscillator model is well adapted. On the other hand, for intramolecular vibrational modes, where the energy differences between the vibrational levels are much larger than that of intermolecular case, Berg et al have observed Raman echo signals (7). This indicates that for such a system, one can apply the stochastic model rather than the Brownian model. Since the Brownian model is also well used in the intravibrational case, one has to investigate the relation between the two models. For such purpose, here we introduce the Brownian model with linear-square system-bath interaction, which is defined by $F_n(Q)=c_nQ^2$ in the Hamiltonian Eq.(1) (Refs. (9-11)). Since the system-bath interaction, $Q^2\Sigma c_nx_n$, is expressed in terms of the creation and annihilation operators of the system, $a$ and $a^+$ as $(a+a^+)(a+a^+)\Sigma c_nx_n$, this interaction causes a level fluctuation due to the terms proportional to $aa^+$ and a $a^+a$. Indeed, the interaction $(aa^++a^+a)\Sigma c_nx_n$ for a two-level system is nothing but the interaction to derive Kubo's stochastic Liouville equation (12). A stochastic Markovian fluctuation corresponds to the spectral density in the following form (8, 12)

$$J(\omega)=\frac{\zeta'\gamma^2}{\gamma^2+\omega^2} \tag{10}$$

The equation of motion for the above spectral distribution with linear-square system-bath interaction can be obtained in the hierarchy form. Then, by solving the equation of motion, we can calculate the 3rd-, 5th- and 7th-order signals (11). Figure 4 presents the 7th-order 2D signal, $I^{(7)}(\tau_1, \tau_2)=|R^{(7)}(\tau_2, 0, \tau_1)|^2$, for the $I_2$ potential used in Section III. Here, we considered the stochastic overdamped case, which had been used to take into account inhomogeneous distribution of vibrational levels (6), and chose the heat bath parameters as (a) $\zeta'=0.1\omega_0$ (b) $\zeta'=0.5\omega_0$, and (c) $\zeta'=\omega_0$ for fixed noise correlation, $\gamma=0.1\omega_0$. In this calculation, we assumed the nonlinear polarizability $\alpha_2$ to be zero and the entire signal is therefore from $\alpha_1^4<[[Q(\tau_1+\tau_2), Q^2(\tau_1)], Q]>$. This signal has the same form as the Raman echo case (6), and we can expect it to be stronger than that of harmonic case, in which the leading order of the signal is $\alpha_1^2\alpha_2^2$. As can be

seen in Fig. 3, echo like peaks arise along the line $\tau_1=\tau_2$ with time period about $1/2\omega_0$=80 (fs). This period becomes shorter for larger $\zeta$', since the effective frequency of potential becomes larger for large frequency modulation. We also observe many peaks corresponding to the two-quantum energy transfer from the system to the bath, which is described by the coupling terms proportional to $a^2$ and $[a^+]^2$ (10). Detailed analysis for $Cs_2$ molecular for different temperatures and coupling strengths will be presented in Refs. (10) and (11).

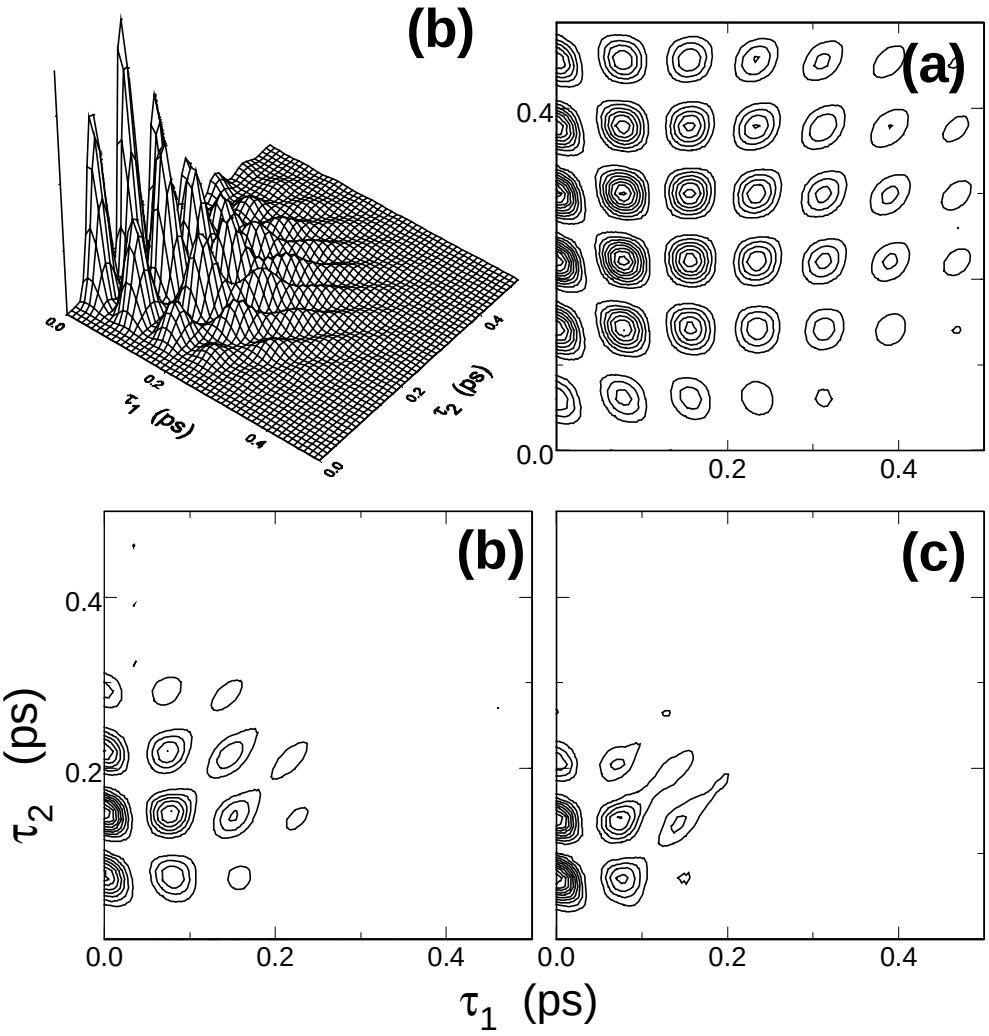


**FIGURE 4.** The 7th-order 2D Raman signal for a harmonic system with nonlinear system-bath interaction for different system-bath coupling (a) $\zeta'=0.1\omega_0$ (b), $\zeta'=0.5\omega_0$, and (c) $\zeta'=\omega_0$. The inverse correlation time of noise is set to $\gamma=0.1\omega_0$. Compared with FIG. 3, Raman echo like peaks along the line $\tau_1=\tau_2$ are prominent.

## V. CONCLUSION

In this paper, we presented the 3rd–, 5th- and 7th-order 2D signals for the harmonic potential and the Morse potential cases for different coupling strengths. We show that, in contrast to the third-order experiments, the 2D signals in 5th- and 7th-order are very sensitive to the shape of the potential. The calculated signals are proportional to the linear polarizability and are expected to be stronger than the harmonic intermolecular vibrational cases. We also calculated the 7th-order 2D signals for Brownian oscillator system with nonlinear system-bath interaction. It was shown that the 7th-order signal in such model has Raman echo like peaks in the overdamped case. Thus, the nonlinear system-bath interaction model can be regarded as a bridge model between a stochastic two-level and Brownian oscillator models.

## ACKNOWLEDGMENTS

Financial support for this work was partially provided by Grand-in-Aid on Priority Area of *Chemical Reaction dynamics in condensed phases* (10206210) and Shimazu Science Foundation.

## REFERENCES

1. Y. Tanimura and S. Mukamel, J. Chem. Phys. **99**, 9496 (1993).
2. K. Okumura and Y. Tanimura, J. Chem. Phys. **105**, 7294 (1996); J. Chem. Phys. **106**, 1687 (1997); J. Chem. Phys. **107**, 2267 (1997); Chem. Phys. Lett. **277,** 159 (1997).
3. Y. Tanimura, Chem. Phys. **233**, 217 (1998).
4. K. Okumura and Y. Tanimura, Chem. Phys. Lett. **278**, 175 (1997).
5. M. Cho, K. Okumura and Y. Tanimura, J. Chem. Phys**. 108**, 1326 (1998); K. Okumura, A. Tokmakoff, and Y. Tanimura, J. Chem. Phys. **111**, 492 (1999).
6. R. F. Loring and S. Mukamel, J. Chem. Phys**. 83**, 2116 (1985).
7. D. Vanden Bout, L. J. Miller, and M. Berg, Phys. Rev. Lett. **67**, 3700 (1991); R. Inaba, K. Tominaga, M. Tasumi, K. A. Nelson, and K. Yoshihara, Chem. Phys. Lett. **211**, 183 (1993).
8. Y. Tanimura and P. G. Wolynes, Phys. Rev. A**43**, 4131(1991); J. Chem. Phys. **96**, 8485 (1992).
9. K. Okumura and Y. Tanimura, Phys. Rev. **E 56**, 2747 (1997).
10. T. Steffen and Y. Tanimura, to be submitted to J. Phys. Soc. Jpn.
11. Y. Tanimura and T. Steffen, to be submitted to J. Phys. Soc. Jpn.
12. Y. Tanimura and R. Kubo, J. Phys. Soc. Jpn, **58**, 101 (1989).